ELSEVIER

Biochimica et Biophysica Acta 1283 (1996) 141–150

BBA Biochimica et Biophysica Acta

Conformational disorder in unsaturated phospholipids by FTIR spectroscopy

Nian-Cherng Chia, Richard Mendelsohn *

Department of Chemistry, Rutgers University, Newark College of Arts and Science, 73 Warren Street, Room 304, Newark, NJ 07102, USA

Received 12 February 1996; accepted 23 April 1996

Abstract

Conformational disorder in liquid alkenes and in the L_α and H_{II} phases of some unsaturated phospholipids has been monitored by FTIR spectroscopy. The CH_2 wagging region (1330–1390 cm^{-1}) in saturated chains contains vibrations of particular 2- and 3-bond conformational states as follows: 1341 cm^{-1}, end-*gauche* (*eg*); 1352 cm^{-1}, double *gauche* (*gg*); 1368 cm^{-1}, the sum of kink and *gtg* states. In unsaturated chains, this spectral region revealed an additional band at 1362 cm^{-1} and (occasionally) a feature near 1348 cm^{-1}. The 1362 cm^{-1} band is tentatively assigned to the wagging of CH_2 groups adjacent to the C = C bond. Substantial populations of both *gg* and (kink + *gtg*) states are evident in the L_α phases of unsaturated phosphatidylcholines (PC's). Unsaturated phosphatidylethanolamines (PE's) are more ordered than their PC counterparts, and possess fewer *gg* and *eg* states. Chain disorder in the H_{II} phase of PE's approaches that in L_α phases of unsaturated PC's. Changes in conformer distributions during the $L_\alpha \rightarrow H_{II}$ transition in 1,2-dioleoylphosphatidylethanolamine (DOPE), 1-palmitoyl,2-oleoylphosphatidylethanolamine (POPE), 1,2-dielaidoylphosphatidylethanolamine (DEPE), and *N*-methyl-DOPE(N-MeDOPE) were semi-quantitatively estimated. For DOPE and DEPE, slight cooperative increases in both *gg* and (kink + *gtg*) states occur, for POPE only the *gg* population increases and for N-MeDOPE only the kink + *gtg* populations increase. These disorder increases are consistent with the small calorimetric ΔH for this transition. Difficulties in quantitative determination of conformational disorder in unsaturated chains are discussed.

Keywords: Phospholipid bilayer; Membrane biophysics; Membrane structure; Phase transition; FTIR

1. Introduction

The phospholipids in native biological membranes are typically characterized by a high percentage of *cis* unsaturation at the acyl chain *sn*-2 position. Despite this fact, the most detailed physical information about phospholipid organization comes from studies of model systems with two saturated chains such as the widely studied 1,2-dipalmitoylphosphatidylcholine (DPPC). One reason for the relative paucity of structural/dynamic data for unsaturated systems is the lack of high resolution X-ray data for these molecules to provide a basis for conformational studies of biologically more relevant disordered phases.

Some thermodynamic and dynamic data are available for bilayers with unsaturated chains. Inclusion of a *cis* C = C bond drastically lowers the gel → liquid crystal phase transition temperature, T_m, the effect being maximal for C = C bonds near the chain center [1]. Differential scanning calorimetry (DSC) [2] reveals transition enthalpies reduced from their saturated counterparts of the same chain length. ^{2}H-NMR [3] studies of 1-palmitoyl,2-oleoylphosphatidylcholine (POPC) reveal that the order parameter profile of the (deuterated) palmitic acyl chain is similar to that for disaturated systems. However, the magnitudes of the order parameters are reduced, suggestive of more conformational disorder in the L_α phase. Acyl chain unsaturation has recently been reported to cause conformational fluctuations of uncertain origin in vesicles [4] and in intact cells of *Acholeplasma laidlawii* enriched in oleoyl chains [5]. To augment the experimental work, molecular mechanics (MM) calculations for POPC [6] and Monte

Abbreviations: DEPE, 1,2-dielaidoylphosphatidylethanolamine; DOPE, 1,2-dioleoylphosphatidylethanolamine; DPPC, 1,2-dipalmitoylphosphatidylcholine; DSC, differential scanning calorimetry; FTIR, Fourier transform infrared; GC-MS, gas chromatography-mass spectrometry; $LiAlH_4$, lithium aluminum hydride; N-MeDOPE, *N*-methyl-1,2-dioleoylphosphatidylethanolamine; POPC, 1-palmitoyl,2-oleoylphosphatidylcholine; POPE, 1-palmitoyl,2-oleoylphosphatidylethanolamine; NMR, nuclear magnetic resonance; THF, tetrahydrofuran.

* Corresponding author. Fax: +1 (201) 6481264.

PII S0005-2736(96)00095-8

Carlo dynamics (MCD) and Brownian dynamics (BD) studies of motions in *cis*-unsaturated hydrocarbon chains [7,8] have recently appeared.

In addition to the gel → liquid crystal transition, unsaturated PE's undergo a transformation to the non-bilayer inverted hexagonal (H_{II}) phase. This polymorphism has led to suggestions of biological functions in which the H_{II} phase may be implicated, such as membrane fusion [9] or membrane-bound enzyme activity [10]. X-ray diffraction has yielded information about lattice structures [11,12] in the hexagonal phase. Acyl chain dynamics have also been probed with ^{2}H-NMR [13,14]. Orientational order of the acyl chains is systematically lower in the H_{II} phase than in the L_α.

Lacking from the above studies is a description of the acyl chain conformational states adopted in disordered phases. Such data would be a useful complement to the molecular modeling approaches and for interpretation of experiments such as NMR and fluorescence spectroscopies which deal with motions slower than *trans-gauche* isomerization, the fastest acyl chain motion.

FTIR spectroscopy has proven useful for identification of chain conformations in saturated alkanes and phospholipid bilayers. Particular two- or three-bond conformational states in disordered phases give rise to localized CH_2 wagging modes absorbing in the 1300–1370 cm^{-1} region as follows; end-*gauche* (*eg*) conformers around the penultimate C-C bond, 1340 cm^{-1}; double *gauche* (*gg*) conformers, 1352 cm^{-1}, and both kink (*gtg'*) and *gtg* states, 1368 cm^{-1} [15]. Band intensities have been quantitatively correlated with these conformations [16–19]. The current study extends in three ways prior investigations (of saturated chains) to the conformational analysis of unsaturated chains. First, complications to the wagging region induced by the C = C bonds are revealed through spectra of liquid alkenes. Second, spectra of 1,2-dioleoylphosphatidylcholine (DOPC) are compared with *cis*-9-octadecene to determine those conformational states which predominate in the L_α phase. Finally, semi-quantitative estimates of the conformational changes that occur during the $L_\alpha \rightarrow H_{II}$ interconversion in some unsaturated PE's are presented.

2. Materials and methods

2.1. Materials

Phospholipids, from Avanti Polar Lipids (Alabaster, AL) and unsaturated fatty acid methyl esters from Sigma (St. Louis MO) were used without purification. Purity was verified in some instances by gas chromatography and DSC. Alcohols (for alkene synthesis) were purchased from NuChek-Prep (Elysian, MN). Tetrahydrofuran (THF) was freshly distilled from sodium and benzophenone (Fluka Chemika-Biochemika, Ronkonkoma, NY) and stored under nitrogen over 4 Å molecular sieves. Both lithium aluminum hydride ($LiAlH_4$) and a sulfur trioxide-pyridine complex were obtained from Aldrich (Milwaukee, WI). Heat transfer fluid was purchased from PolyScience (Niles, IL).

2.2. Synthesis of alkenes

9-*cis*-Octadecene and other alkenes were synthesized from the relevant alcohols via sulfur trioxide-pyridine complexation in THF solution and subsequent $LiAlH_4$ reduction [20]. Product purity was confirmed by GC-MS, NMR and FTIR.

2.3. Sample preparation for FTIR

Phospholipids, dried from $CHCl_3$ solutions, first under a stream of N_2 and then under high vacuum, were dispersed in double distilled H_2O in sealed ampules (usually 4:1 (w/w) H_2O/lipid) at temperatures well above T_m. Samples were incubated for 2–3 h with intermittent agitation to ensure complete hydration. For FTIR thermotropic studies at temperatures greater than 0°C, the aqueous dispersions were contained in a thermostated transmission cell (Harrick Scientific, Ossining, NY) equipped with CaF_2 windows and a 'Teflon'™ spacer of 6 μm thickness. Temperature control was achieved with a Haake circulating water bath. For temperatures between −30°C and 0°C, control was achieved with heat transfer fluid. Temperature was monitored with a digital thermocouple placed adjacent to the point where the IR radiation was focused. Temperature precision is ±0.1°C; temperature accuracy is estimated at ±0.5°C. For the temperature range −100°C to 0°C, samples were housed in a liquid N_2 dewar equipped with external AgCl IR windows. Both the external windows and the cell containing the sample could be individually heated. Temperature regulation was achieved with controlled boil-off of liquid N_2. Typical variation during a run is ±2°C.

2.4. FTIR spectroscopy

FTIR spectra were acquired with a Mattson RS-1 interferometer equipped with a mercury cadmium telluride detector or with a Digilab FTS-40 spectrometer equipped with a deuterated triglycine sulfate detector. Spectra were obtained at ≈4 cm^{-1} resolution, under N_2 purge, by co-addition of 256 interferograms. The resultant interferograms were apodized with a triangular function and Fourier-transformed with one level of zero filling to yield data encoded every ≈2 cm^{-1}. Data from two or three independent preparations were acquired for all samples.

2.5. IR data reduction

For quantitative analysis of CH_2 wagging modes in the 1300–1400 cm^{-1} region, spectra were corrected for any

minor residual water vapor absorption bands, using spectra of the latter recorded under the same conditions of instrument aperture and resolution. Subtraction factors were determined from water vapor bands in the 1900–1980 cm^{-1} region. Following the subtraction process, residual water vapor absorbance in region of interest was less than 10^{-5}. A linear baseline was then selected connecting observed spectral minima between 1329 ± 1 and 1393 ± 1 cm^{-1}. Spectra were transferred to an off-line microcomputer and processed with software supplied by the National Research Council of Canada. To enhance the resolution in this spectral region, a Fourier self-deconvolution procedure with a half-width of 12 cm^{-1} and a K value of 2, was employed [21]. For curve fitting, the spectral bands studied were simulated with mixed Gaussian-Lorentzian functions over the 1329–1393 cm^{-1} spectral range. Initial selection of frequencies was based on literature values for the CH_2 wagging modes as well as for the methyl 'umbrella' (symmetric deformation) mode near 1378 cm^{-1}. Line widths and intensities for the input bands as well as the relative contributions of Gaussian and Lorentzian shapes to the entire set of bands (treated as a single parameter) were allowed to vary during the computation. The intensities of the individual wagging modes were ratioed to the methyl umbrella mode to produce the relative intensities used in calculations.

The CH_2 stretching modes are in a spectral region (2800–3100 cm^{-1}) which lies on a slope of the liquid H_2O stretching vibration. To compensate for this feature, a liquid water spectrum collected under the same conditions as the sample spectrum was subtracted. Peak positions of the symmetric (≈ 2850 cm^{-1}) and asymmetric (≈ 2920 cm^{-1}) CH_2 stretching modes were determined with a center of gravity algorithm [22].

3. Results

3.1. Liquid alkenes

IR absorbance and deconvolved spectra for liquid 9-*cis*-octadecene in the CH_2 wagging region (≈ 1330–1390 cm^{-1}) are presented in Fig. 1 A and B, respectively. This chain length is the focus of the current study as oleoyl chains are amongst the most common in native membranes. Spectra at several temperatures between 20 and 85°C are overlaid, offset from one another. The strongest band in this spectral region arises from the symmetric methyl deformation ('umbrella') mode at 1378 cm^{-1}. Although the absorbance data (Fig. 1A) are broad, bands at ≈ 1341 and 1351 cm^{-1} are readily observed and assigned to *eg* and *gg* modes. Resolution enhancement of the contour by Fourier self-deconvolution (Fig. 1B) reveals the presence of a previously unidentified feature (present as a shoulder) at 1362 cm^{-1} in addition to the 1368 cm^{-1} (kink + *gtg*) mode. A possible additional feature in the *gg*

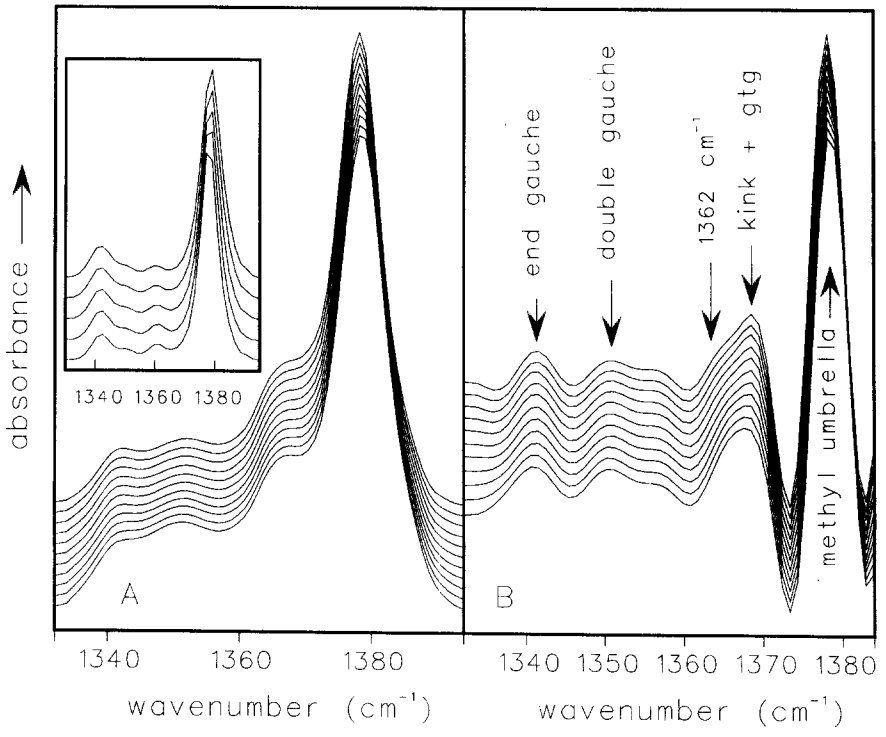

Fig. 1. (A) IR absorbance spectra for 9-*cis*-octadecene at various temperatures. Eleven (11) spectra are offset for clarity and are presented from bottom (35°C) to top (85°C) in intervals of ≈ 5 K. (Inset: IR absorbance data of 5-*cis*-decene at 5.3, 27.3, 45.8, 65.5 and 80.4°C, from bottom to top. Note the intense feature at 1361 cm^{-1}) (B) Deconvolved IR spectra for 9-*cis*-octadecene at various temperatures. Presented as in (A). Bands arising from particular vibrational modes are marked. Note the shoulder at ≈ 1362 cm^{-1}.

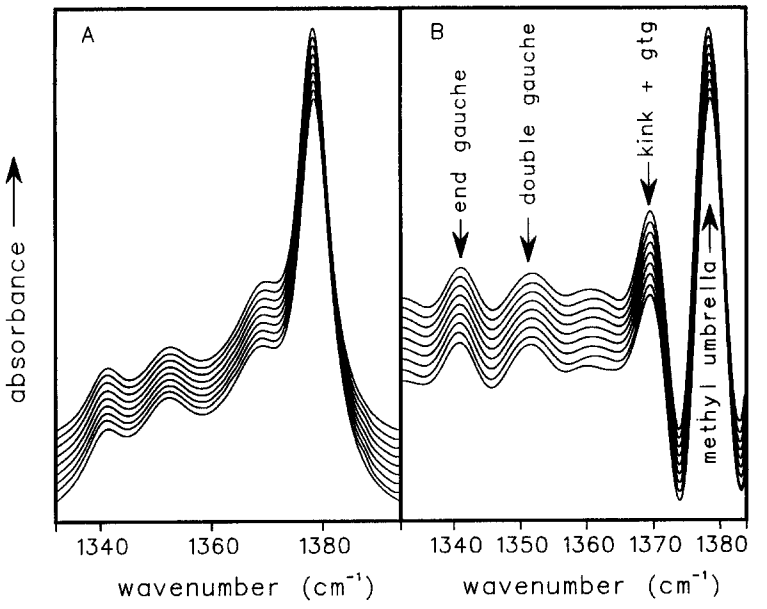

Fig. 2. (A) IR absorbance spectra for octadecane. Nine (9) spectra are offset for clarity and were collected (bottom to top) at 27.7, 34.8, 40.6, 48.2, 56.1, 65.5, 75.9, 83.4, 91.9°C, respectively. (B) Deconvolved IR spectra octadecane at various temperatures. Presented as in (A). Bands arising from particular vibrational modes are marked. Note the absence of intensity at 1362 cm^{-1}.

region is also detected as a weak peak at $\approx$ 1358 cm^{-1} in addition to the major component. The association of the feature at 1362 cm^{-1} with wagging modes from methylene groups adjacent to the C = C bond is made plausible by examination of original (undeconvolved) spectra of 5-*cis*-decene (inset in Fig. 1A). The relatively short chain lengths on either side of the C = C bond preclude the extensive formation of kink + *gtg* conformers with their concomitant IR intensity at 1368 cm^{-1}. The appearance of a band at 1362 cm^{-1} is evident in the inset and does not require resolution enhancement of the data. The necessity to deconvolve longer chain IR data (Fig. 1B) arises as their spectra naturally contain greater contributions from kink + *gtg* sequences leading to intensity at 1368 cm^{-1} that overlaps the 1362 cm^{-1} band.

For comparison with saturated species, absorbance and deconvolved spectra of octadecane are shown in Fig. 2 A and B, respectively. The four expected features (three wagging modes and the methyl umbrella mode) are evident, with no significant band occurring at 1362 cm^{-1} either in the raw absorbance or resolution-enhanced data. These data offer support to the assignment of the 1362 cm^{-1} mode to the wagging of CH_2 groups adjacent to the C = C bond.

3.2. Phospholipids

The presence of a previously unidentified feature at 1362 cm^{-1} in 9-*cis*-octadecene (and in all other long chain alkenes in the range C_{16}–C_{24}) led us to search for this band in unsaturated phospholipids. Deconvolved spectra of

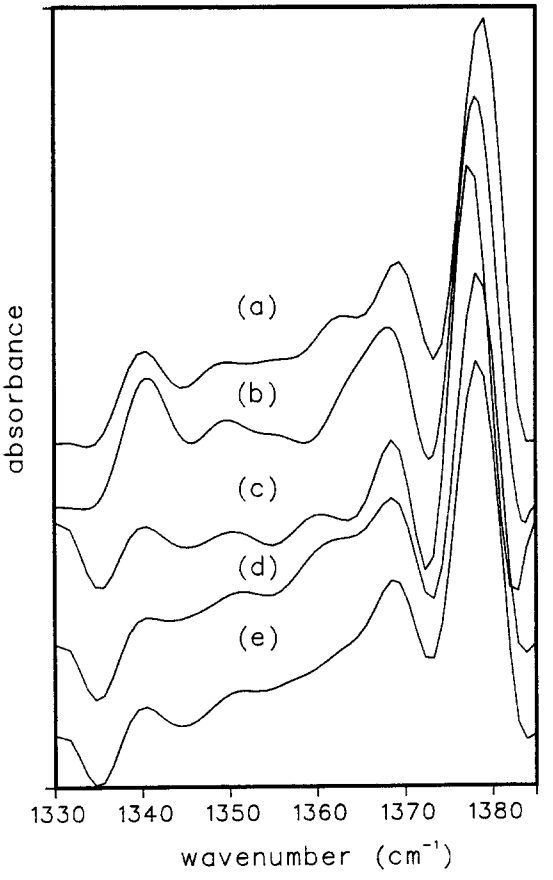

Fig. 3. Deconvolved spectra of phospholipids in the CH_2 wagging region. (a) DOPC: 91.8°C, L_α phase; (b) 1,2-dierucoylPC: 87.1°C, L_α phase; (c) DOPE: 30.3°C, H_{II} phase; (d) N-MeDOPE: 86.4°C, H_{II} phase; (e)POPE: 89.9°C, H_{II} phase. Note the peaks/shoulders in the 1361–1365 cm^{-1} region of a–d.

the wagging region for five phospholipid molecules in both the L_α and H_{II} phases are shown in Fig. 3. It is noted that in the raw absorbance data (not shown), the 1368 cm^{-1} band occasionally has a shoulder on its low frequency side, but a clear peak a 1362 cm^{-1} is hardly ever observed. This observation is consistent with the data in Fig. 1, which suggests that the presence of the relatively long sequences of CH_2 groups permits the formation of conformers that absorb at 1368 cm^{-1}, thereby obscuring the underlying and overlapped 1362 cm^{-1} feature. For DOPC and 1,2-dierucoylPC (L_α phases), DOPE and N-MeDOPE (H_{II} phases), the deconvolved spectra reveal bands in this region whose frequency varies from a well defined feature at $\approx$ 1360 cm^{-1} to a shoulder several wavenumbers higher. For H_{II} phase POPE in Fig. 3e no band is resolved, though some underlying intensity may be present. In addition to the appearance of the 1362 cm^{-1} band, an additional feature in the vicinity of the *gg* mode is occasionally manifest as a doublet at $\approx$ 1348, 1354 cm^{-1}. These can best be discerned for the PC's; we reiterate that the identification is tentative.

In prior studies of two or three bond conformational disorder in disaturated phospholipids [17], wagging mode intensities were compared to those of alkanes of the same chain length. A similar procedure was adopted in the present work, with alkenes as the reference standard. To determine the contribution of each spectral feature (including the 1362 cm^{-1} and 1348 cm^{-1} bands, if needed) to the original contour, curve-fitting analyses using band positions determined from second derivative spectroscopy was carried out. Typical results are demonstrated in Fig. 4 for H_{II} phase N-MeDOPE at 89.7°C. The difference between the original contour (solid line) and the sum of the constituent bands (dashed lines) is small (random deviations between calculated and observed spectra less than 1% across the contour) and is typical of the quality of data

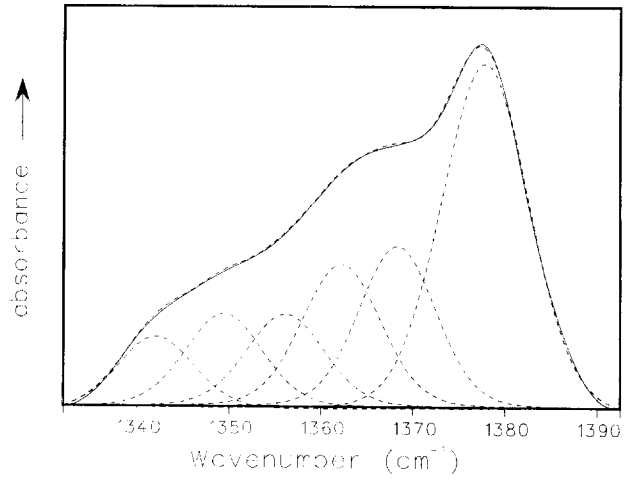

Fig. 4. Curve-fitting of the N-MeDOPE spectrum (89.7°C) in the CH_2 wagging region. Six bands were used in the fit. Original spectrum, (————); individual bands and their sum, (– – –).

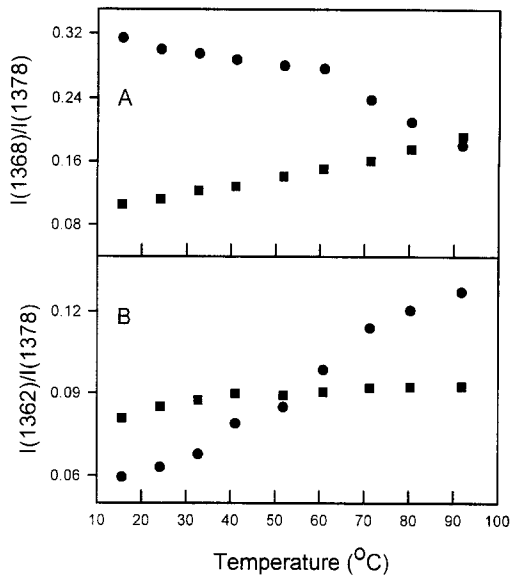

Fig. 5. (A) Temperature dependence of the relative intensity for the 1368 cm^{-1} (kink+ *gtg*) marker band for 9-*cis*-octadecene (●) and for DOPC (■). (B) Temperature dependence of the relative intensity for the 1362 cm^{-1} band for 9-*cis*-octadecene (●) and for DOPC (■).

reduction protocols. Thus, these six bands provide an adequate representation of the DOPE wagging contour. For some systems, inclusion of the 1348 cm^{-1} band does not improve the fit and is omitted.

For determination of conformational order, the band intensities of the conformation marker bands at 1368, 1362, 1352, 1348, and 1341 cm^{-1}, normalized to the 1378 cm^{-1} intensity, are plotted for DOPC and for 9-*cis*-octadecene in Figs. 5 and 6. For comparative purposes, the

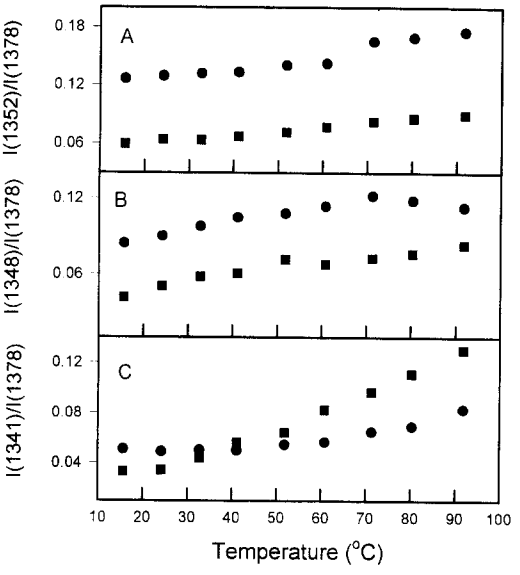

Fig. 6. (A) Temperature dependence of the relative intensity for the 1352 cm^{-1} (*gg*) marker band for 9-*cis*-octadecene (●) and for DOPC (■). (B) Temperature dependence of the relative intensity for the 1348 cm^{-1} marker band for 9-*cis*-octadecene (●), and for DOPC (■). (C) Temperature dependence of the relative intensity for the 1341 cm^{-1} (*eg*) marker band for 9-*cis*-octadecene (●), and for DOPC (■).

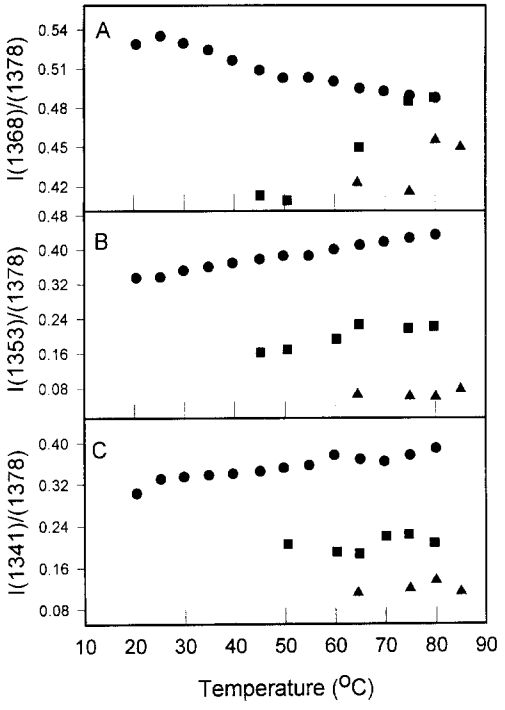

Fig. 7. (A) Temperature dependence of the relative intensity for the 1368 cm^{-1} (kink + *gtg*) marker band for hexadecane (●), for DPPC (■), and for DPPE (▲). (B) Temperature dependence of the relative intensity for the 1353 cm^{-1} (*gg*) marker band for hexadecane (●), for DPPC (■), and for DPPE (▲). (C) Temperature dependence of the relative intensity for the 1341 cm^{-1} (*eg*) marker band for hexadecane (●), for DPPC (■), and for DPPE (▲).

intensity ratios for the phospholipids have been halved (except for the *eg* mode) to account for the fact that there is only one methyl group/chain in the phospholipids. The intensity of the 1368 cm^{-1} band for the alkene (Fig. 5A) is seen to decrease with temperature. This is a non-intuitive result, since the number of kink + *gtg* states is expected (from theories such as the rotational isomeric state (RIS) model [23]) to increase with temperature. A similar result has been observed for a series of saturated alkanes [17]. For DOPC, the expected temperature dependence at 1368 cm^{-1} is noted. The intensities of the other conformation markers increase more or less monotonically with increasing temperature. For comparison, the 1368, 1353, and 1341 cm^{-1} bands for DPPC and DPPE (L_α bilayer phases) are compared with the data for hexadecane in Fig. 7 A–C.

3.3. The $L_\alpha \rightarrow H_{II}$ interconversion in DOPE and N-MeDOPE

The thermotropic behavior of the CH_2 symmetric stretching band near 2850 cm^{-1} is shown in Fig. 8 for DOPE. This parameter qualitatively monitors acyl chain conformational disorder, the frequency increasing as disorder is introduced. The main gel → liquid crystal transition, as revealed by a ≈ 1.6 cm^{-1} increase, appears between −7 and −5°C, in good agreement with literature values [12]. A second transition is evident at approx. 8–10°C, also in accord with the literature value for the $L_\alpha \rightarrow H_{II}$ transition [24]. The frequency increase for this transition is small (0.2–0.3 cm^{-1}), but is consistently observed, and demonstrates the precision of FTIR (for a previous IR study of $L_\alpha \rightarrow H_{II}$ interconversion using this parameter, see [25]). The discontinuity near 0°C arises from the effect of changed spectral background on the measured frequency when the ice in the sample melts and is not a lipid structural transition.

Figs. 9 and 10 present the intensities (determined from curve fitting) of the various wagging modes for DOPE and

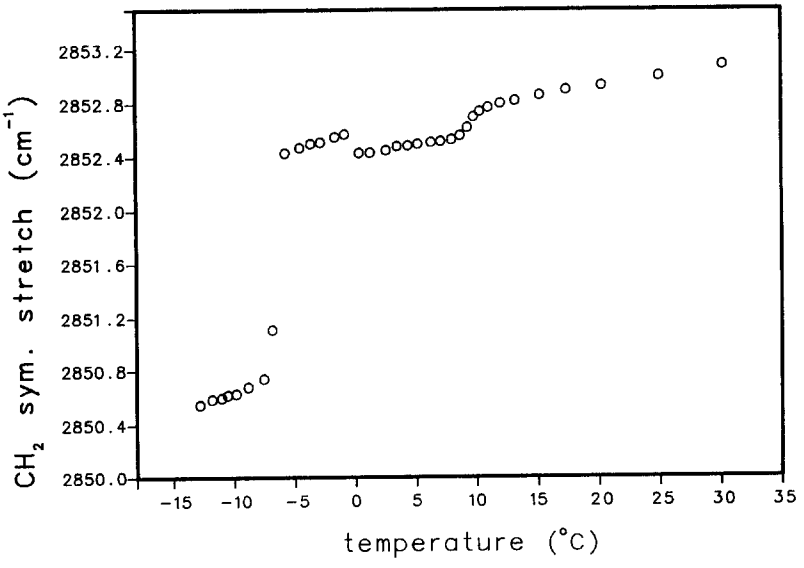

Fig. 8. Temperature dependence of the CH_2 symmetric stretching frequency for DOPE. The gel-liquid crystal transition is detected at ≈ −7°C, while the L_α–H_{II} transition is centered at 8–9°C. The slight decrease, evident as a discontinuity at ≈ 0°C, arises from the effect of changed spectral background on the measured frequency when the ice in the sample melts and is not a lipid structural transition.

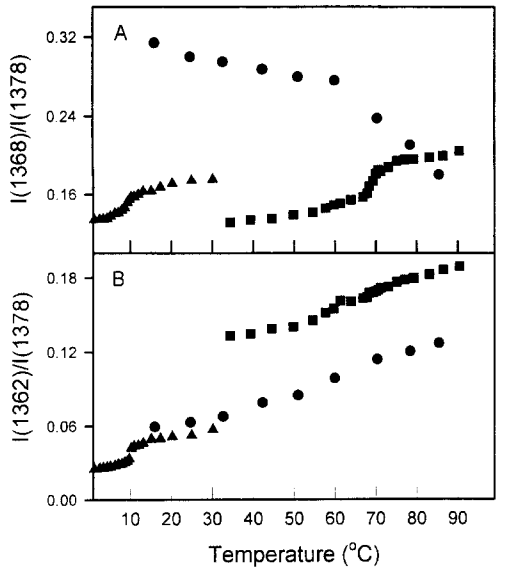

Fig. 9. (A) Temperature dependence of the relative intensity for the 1368 cm^{-1} (kink + *gtg*) marker band for 9-*cis*-octadecene (●), for N-MeDOPE (■), and for DOPE (▲). (B) Temperature dependence of the relative intensity for the 1362 cm^{-1} band for 9-*cis*-octadecene (●), for N-MeDOPE (■), and for DOPE (▲).

N-MeDOPE compared with 9-*cis*-octadecene. Equivalent data (not shown) have been collected for DEPE and POPE. For DOPE as noted above, the 1348 cm^{-1} intensity was negligible, thus this feature was not included in the curve-fitting. The bands at 1368 and 1353 cm^{-1} (Fig. 9A and Fig. 10A) show discontinuities at the L_α–H_{II} transition, thereby revealing increases in the (kink + *gtg*) and *gg* populations, respectively. In contrast, the 1341 cm^{-1} band (Fig. 10C) shows at most only a small discontinuity at this transition. The 1362 cm^{-1} band (Fig. 9B) also undergoes a cooperative intensity increase.

N-MeDOPE has a higher $L_\alpha \rightarrow H_{II}$ transition range (65–70°C) than DOPE, consistent with its substantially larger headgroup. The temperature profiles of the wagging mode intensities differ significantly from those for DOPE in that the only vibration to demonstrate a substantial discontinuous change during the transition is the (kink + *gtg*) marker band (Fig. 9A). For POPE, the *gg* marker band alone shows a cooperative increase, while for DEPE both the *gg* and (kink + *gtg*) populations increased during this transition (data not shown in either case).

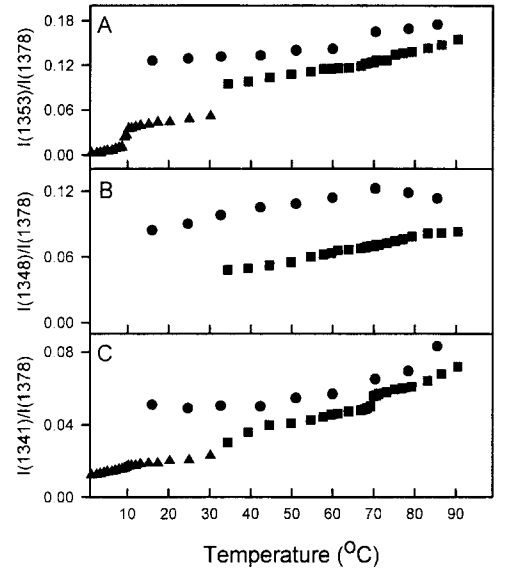

Fig. 10. (A) Temperature dependence of the relative intensity for the 1353 cm^{-1} (*gg*) marker band for 9-*cis*-octadecene (●), for N-MeDOPE (■), and for DOPE (▲). (B) Temperature dependence of the relative intensity for the 1348 cm^{-1} marker band for 9-*cis*-octadecene (●), for N-MeDOPE (■), and for DOPE (▲). (C) Temperature dependence of the relative intensity for the 1341 cm^{-1} (*eg*) marker band for 9-*cis*-octadecene (●), for N-MeDOPE (■), and for DOPE (▲).

4. Discussion

4.1. Complications for quantitative analysis

Conversion of the intensities in Figs. 5–7, 9 and 10 to conformational populations is complicated by several factors compared with the analysis of saturated chains. For saturated systems, the RIS model is used to generate conformational statistics for the reference alkane. The measured alkane intensities are then compared with those of the phospholipids to determine conformational states in the latter. A qualitative example of the process is shown in Fig. 7B. The population of *gg* states in DPPC (above T_m) is about 1/2 of that in liquid hexadecane. This is a direct measure of bilayer-induced constraints to conformational disordering. A further decrease of a factor of 2–3 is seen in this intensity in going from DPPC to DPPE. This decrease directly monitors the tighter chain packing that results from the smaller PE headgroup. The main source of conformational disordering in DPPC or DPPE is the sum of kink + *gtg* states measured by the 1368 cm^{-1} intensity (Fig. 7A). The intensity of this mode is at least 70% of that in alkanes.

Extension of these procedures to unsaturated chains is hampered in several ways. First, the conformations and the conformational energetics of the C-C bonds adjacent to the double bond are not well determined. From microwave [26] and NMR studies for gaseous 1-butene [27], two dominant conformers, the *cis* and *skew* forms, were shown to co-exist. The energy difference between them is small, 150 ± 150 cal, with the *skew* form more stable. In contrast, other vibrational spectroscopic [28] and NMR studies [29] concluded that the *cis* conformer is more stable by 100 ± 50 cal/mol.

Experimental extensions of these (somewhat contradictory) gas phase results to molecules more relevant to phospholipids are sparse. One study [30] identified two

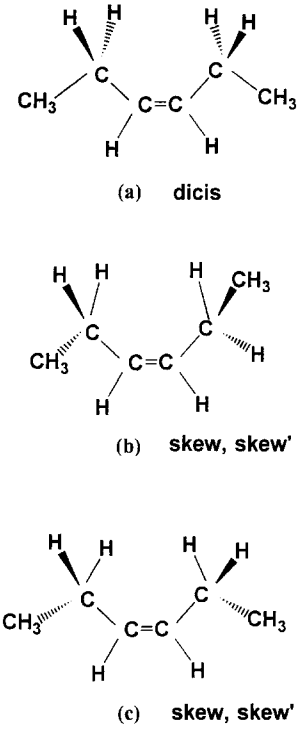

Fig. 11. The (a) di*cis*, (b) *skew-skew* and (c) *skew-skew'* conformers, illustrated for *cis*-3-hexene.

crystalline forms in the Raman spectra of solid oleic acid corresponding to the (*skew,skew*) and (*skew,skew'*) states. These had melting points of 13°C and 16°C. The structures are depicted for *cis*-3-hexene along with the energetically less likely di*cis* conformation in Fig. 11.

The lack of crystal structure data and the uncertainty as to the conformational states that occur for unsaturated phospholipids has led investigators to rely on computer simulations to deduce the effects of introducing a C = C bond into the middle of an isolated all-*trans* chain (i.e. the gel state of the molecule). MM calculations for POPC [6] suggest that *skew* conformations of the carbon skeleton are widely adopted in unsaturated alkenes. The calculations reveal thirteen types of nearly isoenergetic structure motifs in the neighborhood of this bond. Some conformations near the C = C bond containing kinks appear to be readily interconvertible, as the two C-C bonds adjacent to the double bond are highly flexible. Kink-like sequences of the form $t\Delta s^- g^+$, $g^+ s^+ \Delta s^+$, $s^+ \Delta s^+ g^+$ (Δ is the C = C bond and s^+, s^- are *skew* forms with opposite rotational senses), were all calculated to be of similar energy (energy differences between them $< \approx 3\ kT$). Depending on barrier heights, these states will coexist and interconvert. Similar considerations probably apply to the L_α phase, although no detailed modeling has been found by the authors for this phase for unsaturated systems. These conformations produce additional possibilities compared with saturated chains for the wagging mode frequency of the methylenes adjacent to the double bond. It is anticipated that the CH_2 wagging frequency for any of these sequences would be close to 1368 cm^{-1}; thus the 1362 cm^{-1} band is very tentatively assigned to any or all of these conformer states. Such an assignment is consistent with the data in Fig. 1. However, this assignment is very difficult to prove without an extensive set of derivatives providing experimental data from which to generate an accurate force field for unsaturated molecules.

In addition to uncertainty about the conformations of the C-C bonds adjacent to the C = C bonds in alkenes, the applicability of the RIS model to each half of the acyl chain is untested. In bilayer states, one might guess that the half of the acyl chain toward the center of the bilayer has a different distribution of conformational order than that in the polar region, consistent with Raman data [31].

Table 1
Cooperative changes in 2- or 3-bond conformational states for unsaturated PE derivatives during the $L_\alpha \rightarrow H_{II}$ transition

Molecule	T_{ho} [a] (°C)	T_{hc} [b] (°C)	Conformer	Δ conformer [c]	ΔH [d] (cal/mol)	ΔH_{conf} [h] (cal/mol)
DOPE	8.7	11	*gg*	0.117	300 [e]	≈ 150
			kink + *gtg*	0.029		
POPE	65.9	70.6	*gg*	0.042	250 [f]	≈ 40
DEPE	62.0	65.0	kink + *gtg*	0.043	250 [f]	≈ 100
			gg	0.061		
N-MeDOPE	61.0	65.7	kink + *gtg*	0.044	250 [g]	≈ 40

[a] Onset temperature for $L_\alpha \rightarrow H_{II}$ transition.
[b] Completion temperature for $L_\alpha \rightarrow H_{II}$ transition.
[c] Changes in the number of the indicated conformers over the indicated temperature interval; changes are calculated from the RIS model with $E_g = 500$ cal/mol.
[d] As determined from DSC data.
[e] Gawrisch et al. [32].
[f] Current study.
[g] Siegel et al. [33].
[h] Enthalpy change due to increased conformational disorder. Calculated from the sum of cooperative changes in IR marker band intensities. This is a semi-quantitative value and has been rounded off to 1 or 2 significant figures. See text for details.

Thus any IR-determined conformations for each two- or three-bond conformer will report the sum of the behavior in each half of the phospholipid acyl chains.

The appearance of new spectral features derived from unknown conformational states creates problems with the quantitative analysis of the IR data. The band at 1348 cm^{-1} in DOPC probably affects the intensity (as determined from curve-fitting) of the neighboring 1353 cm^{-1} band, so that the latter is much reduced in alkenes vs. alkanes (compare Fig. 6A,B with Fig. 7A). Similar comments pertain to the 1362 cm^{-1} band. In addition, although it is tacitly assumed that the new feature(s) in the wagging regions arise from CH_2 wagging modes of the methylenes adjacent to the double bond, this is not necessarily true. For example, the presence of the C = C bond may create kinks or *gg* states in the rest of the chain with geometries that are slightly distorted from the norm. These new geometries may create wagging frequencies slightly shifted from 1368 or 1353 cm^{-1}.

Even under the above limitations, it is feasible to semi-quantitatively estimate *changes* (rather than the absolute levels) in the population of particular two- or three-bond populations during the L_α–H_{II} interconversion. The calculation assumes that E_g (the energy of a *gauche* bond relative to a *trans* in those chain regions away from the C = C bond) is 500 cal. The RIS model is applied separately to the methylene sequences on either side of the C = C bond for the alkene. The results are shown in Table 1 and are relatively independent (± 5%) of the conformation of the C-C adjacent to the C = C bond in the chain. Included in Table 1 are ΔH data for the transitions as determined calorimetrically.

4.2. Acyl chain conformations in unsaturated lipids

Despite limitations to quantitative analysis noted above, several conclusions may be drawn from the current experiments. In prior studies of conformational changes in disaturated PC's [16,17], the kink + *gtg* conformer set was shown to be the dominant form of conformational disordering, and the presence of *gg* states fairly minor. Similar effects were noted for DOPC, although a smaller proportion of kink + *gtg* states (at low temperatures) is observed for the latter. This diminution may be related to artifacts of curve-fitting, i.e. the effects of the 1362 cm^{-1} band on the kink + *gtg* marker band intensity. At low temperatures, both *gg* and (kink + *gtg*) states are responsible for disordering in DOPC, whereas at high temperatures a greater proportion of the disordering is from (kink + *gtg*) forms. We speculate that the *gg* states dominate in the lower half of the chain and are relatively unaffected by temperature.

The *eg* and *gg* populations in the L_α phase of DOPE (Fig. 10 A, C) are much reduced from those for DOPC (Figs. 5 and 6), a result similar to that observed for the saturated chains (Fig. 7). In addition, kink + *gtg* forms are present at similar levels in both cases. Above the $L_\alpha \rightarrow H_{II}$ transition for DOPE, the populations of the *gg* and *eg* states, and approach those of L_α phase DOPC.

4.3. Determination of conformational changes during the L_α–H_{II} interconversion

The populations of *gg* and (kink + *gtg*) states increase by about 0.12 and 0.028 per chain, respectively, during the $L_\alpha \rightarrow H_{II}$ transition in DOPE (Table 1). If E_g is assumed to be 500 cal/mol, then these increases involve an enthalpy change of roughly 150 cal/mol (note that one *gg*, kink or *gtg* state involves the formation of two *gauche* bonds). Considering the approximations and assumptions involved, this estimate is at best semi-quantitative, but is at least in line with the low measured calorimetric enthalpy of 300 cal/mol. Similar values deduced for the other molecules are listed in Table 1. It is evident that not all the enthalpy change arises from chain disordering. Hydration state changes and headgroup rearrangements certainly produce additional contributions [32].

Conformational disorder for N-MeDOPE is much greater than in DOPE, a consequence of the larger headgroup in the former. This enhanced disordering (evident from the curve-fitting results in Figs. 3 and 4) is manifest by increased *gg*, *eg*, and 1348 cm^{-1} intensities in N-MeDOPE, when the same phases are compared (see Fig. 10). The larger headgroup also delays the onset of the $L_\alpha \rightarrow H_{II}$ transition. The inherent occurrence of greater disorder in the acyl chains of N-MeDOPE may explain the differences observed in the thermotropic behaviors at this transition for the two molecules. Large increases in the 1368, 1362 and 1353 cm^{-1} bands are seen for DOPE, whereas only the first of these increases cooperatively for N-MeDOPE. The 1353 cm^{-1} band already exhibits substantial intensity in the bilayer phase of N-MeDOPE, so that the constraints to *gg* forms in L_α DOPE are alleviated for N-MeDOPE.

Acknowledgements

This work was supported by US PHS grant GM-29864 to R.M. We thank Drs. Robert Snyder and Luke Liang at the University of California (Berkeley) for DSC determinations of the enthalpy changes during the bilayer–hexagonal transitions of POPE and DEPE.

References

[1] Barton, P.G. and Gunstone, D. (1975) J. Biol. Chem. 60, 4470–4476.
[2] Wang, Z.-Q., Lin, H.-N., Li, S. and Huang, C.-H. (1995) J. Biol. Chem. 270, 2014–2023.
[3] Seelig, A. and Seelig, J. (1977) Biochemistry 16, 45–50.
[4] Litman, B.J., Lewis, N. and Levin, I.W. (1991) Biochemistry 30, 313–319.
[5] Moore, D.J., Gericke, A. and Mendelsohn, R. (1996) Biochim. Biophys. Acta 1279, 49–57.

[6] Li, S., Lin, H.-N., Wang, Z.-Q. and Huang, C. (1994) Biophys. J. 66, 2005–2018.
[7] Levine, Y.K., Kolinski, A. and Skolnick, J. (1991) J. Chem. Phys. 95, 3826–3834.
[8] Rey, A., Kolinski, A., Skolnick, J.L. and Levine, Y.K. (1992) J. Chem. Phys. 97, 1240–1249.
[9] Verkleij, A.J. (1984) Biochim. Biophys. Acta 799, 43–63.
[10] Navarro, J., Toivio-Kinnucan, M. and Racker, E. (1984) Biochemistry 23, 130–135.
[11] Seddon, J.M., Cevc, G., Kaye, R.D., and Marsh, D. (1984) Biochemistry 23, 2634–2644.
[12] Gruner, S.M., Tate, M.W., Kirk, G.L., So, P.T., Turner, D.C., Keane, D.T., Tilcock, C.P.S. and Cullis, P.R. (1988) Biochemistry 27, 2853–2866.
[13] Sternin, E., Fine, B., Bloom, M., Tilcock, C.P.S., Wong, K.F. and Cullis, P.R. (1988) Biophys. J. 54, 689–694.
[14] Lafleur, M., Cullis, P.R. and Bloom, M. (1990) Eur. Biophys. J. 19, 55–62.
[15] Snyder, R.G. (1967) J. Chem. Phys. 47, 1316–1380.
[16] Casal, H.L. and McElhaney, R.N. (1990) Biochemistry 29, 5423–5427.
[17] Senak, L., Davies., M.A. and Mendelsohn, R. (1991) J. Phys. Chem. 95, 2565–2571.
[18] Tuchtenhagen, J., Ziegler, W. and Blume, A. (1994) Eur. J. Biophys. 23, 323–335.
[19] Doebler, R.W., Steggles, A.W. and Holloway, P.W. (1995) Biophys. J. 68, A429.
[20] Corey, E.J. and Achiwa, K. (1969) J. Org. Chem. 34, 3667–3668.
[21] Kauppinen, J.K., Moffatt, D.J., Mantsch, H.H. and Cameron, D.G. (1981) Anal. Chem. 53, 1454–1457.
[22] Cameron, D.G., Kauppinen, J.K., Moffatt, D.J. and Mantsch, H.H. (1982) Appl. Spectrosc. 36, 245–249.
[23] Flory, P.J. (1969) Statistical Mechanics of Chain Molecules, Wiley, New York.
[24] Lewis, R.N.A.H., Mannock, D.A., McElhaney, R.N., Turner, D.C. and Gruner, S.M. (1989) Biochemistry 28, 541–548.
[25] Mantsch, H.H., Martin, A. and Cameron, D.G. (1981) Biochemistry 20, 3138–3145.
[26] Kondo, S., Hirota, E. and Morino, Y. (1968) J. Mol. Spectrosc. 28, 471–489.
[27] Bothner-By, A.A. and Naar-Colin, C. (1961) J. Am. Chem. Soc. 83, 231–236.
[28] Durig, J.R. and Compton, D.A.C. (1980) J. Phys. Chem. 84, 773–781.
[29] Woller, P.W. and Garbisch, E.W., Jr. (1972) J. Org. Chem. 37, 4281–4285.
[30] Koyama, Y. and Ikeda, K.-I. (1980) Chem. Phys. Lipids 26, 149–172.
[31] Lippert, J.L. and Peticolas, W.L. (1972) Biochim. Biophys. Acta 282, 8–17.
[32] Gawrisch, K., Parsegian, V.A., Hadjuk, D.A., Tate, M.W., Gruner, S.M., Fuller, N.L. and Rand, R.P. (1992) Biochemistry 31, 2856–2864.
[33] Siegel, D.P., Banschbach, J. and Yeagle, P.L. (1989) Biochemistry 28, 5010–5019.